Article

Journal of Nanoscience and Nanotechnology
Vol. 16, 10927–10934, 2016
www.aspbs.com/jnn

Fluorescent Nanostructures from Aromatic Diblock Copolymers via Atom Transfer Radical Polymerization

Jungmok You[1] and Eunkyoung Kim[2,*]

[1]Department of Plant and Environmental New Resources, Kyung Hee University, 1732 Deogyeong-daero, Giheung-gu, Yongin-si, Gyeonggi-do 446-701, South Korea
[2]Department of Chemical and Biomolecular Engineering, Yonsei University, 50 Yonsei-ro, Seodaemun-gu, Seoul 120-749, South Korea

Well-defined fluorophore (anthracene or pyrene) containing copolymers were synthesized via atom transfer radical polymerization (ATRP) using methyl methacrylate (MMA) and fluorophore bound methacrylate (AntMA or PyMA). The copolymers exhibited clearly distinct thermal and optical properties, in terms of glass transition temperature (T_g) and emission spectrum, depending on the polymer structures. Moreover self-assembly properties of the copolymers affected the formation of the polymer nanostructures at condensed phase, to distinguish the random against block copolymers. The antracene containing random copolymer had a single T_g value while antracene containing block copolymer had two T_g values. In addition, sharp fluorescence peaks (398, 416 and 439 nm) werer observed in the random copolymer of antracene. In contrast, the anthracene containing block copolymer showed a broad tailing of the peak reaching ~550 nm. Interestingly, the copolymers having both randomly distributed anthracene units and consecutively connected pyrene units exhibited sharp emission at 398, 416, and 442 nm originated from the antracene unit and pyrene excimer emission at 482 nm. More importantly, well ordered nanopore films and nano scale micelle structures, originated from the self-assembly of antracene or pyrene block unit, were formed in block copolymers, while any type of an ordered structure was not found from the random copolymers. Therefore fluorescent nanostructures could be well-controlled by the polymers structures containing antracene and pyrene units, which might be widely useful for the development of novel photonics, optoelectronics, and sensor devices.

Keywords: Fluorescent Polymer, Diblock Copolymer, Nanostructures, Self-Assembly, Atom Transfer Radical Polymerization.

1. INTRODUCTION

The self-assembly of soft materials have garnered considerable attention as an attractive means of generating nanoscale structures and patterns.[1,2] Various block copolymers and liquid crystals leading to thermodynamically-ordered nanostructures have been extensively exploited for applications including separation technology, catalysis, sensors, photonics, and optoelectronics.[3–7] A number of laboratories, including our own, have been conducting molecular design and synthesis of functional materials to modulate their physicochemical and optoelectronic properties as well as to fabricate self-assembled nanostructures.[8–15] Fluorescent materials, widely used for biosensors, displays, and photonic devices, have been readily synthesized and processed as nanoscale structures for their specific applications. However, the self-assembled fluorescent nanostructure of block copolymers has been much less explored relative to that of fluorescent dye-doped nanoparticles, fluorescent polyelectrolytes, and quantum dots.

Anthracene, a fluorophore, is a promising building block for highly fluorescent organic materials in order to fabricate organic semiconductors and electroluminescent devices.[16,17] Thus, antracene containing polymers have received considerable attention due to their attractive features such as the versatile photo-reactivity and various photonic applications.[17–19] Our laboratory previously described the facile one-pot synthesis of a

*Author to whom correspondence should be addressed.

 1533-4880/2016/16/10927/008 doi:10.1166/jnn.2016.13266

photo-patternable Ant polymer and the separate catalytic polymerization of Ant in a nanoporous reactor by Friedel–Crafts alkylation reactions.[20, 21]

Herein, we report the synthesis of antracene and pyrene containing random and diblock copolymers via atom transfer radical polymerization (ATRP) and the self-association properties of the polymers for the formation of nanostructures. In the random copolymers, the fluorephoreacent AntMA units are connected to methyl nmethacrylate (MMA) units by covalent chemical bonding, but AntMA and MMA units are randomly connected. On the other hand, in the AntMA containing diblock copolymers, AntMA units connected consecutively to form AntMA block, which was connected to PMMA macromere. The random copolymer of MMA and AntMA can be connected further to pyrene polymer in which fluorophorescent pyrene units are connected consecutively to form blocks.

The controlled/living radical polymerization by ATRP, which has emerged as one of the most active fields in polymer chemistry, provides new possibilities for designing and engineering complex polymer materials. This polymerization method allows for the design of chemical structures of each segment and controls the chain length, composition, and polydispersity. We generated fluorescent nanoscale structures by self-assembly of block copolymers containing either anthracene or pyrene and also explored the emission properties of the random and block copolymers containing fluorophores.

2. EXPERIMENTAL DETAILS

2.1. Materials

Methyl methacrylate (MMA, Aldrich, 99%) was obtained from Aldrich and was passed through a column of basic alumina and then distilled prior to polymerization. 9-Anthracenemethanol, 1-pyrenemethanol, triethylamine, anisole, methacryloyl chloride, Cu(I)Br, $CuBr_2$, Cu(I)Cl, $CuCl_2$, *N*,*N*,*N*′,*N*″,*N*″-pentamethyldiethylenetriamine (PMDETA, 99%, Aldrich), and ethyl-2-bromo isobutyryl bromide (EbiB) were obtained from Aldrich and used as received.

2.2. Instruments

The molecular weight and polydispersity were determined by gel permeation chromatography (GPC). The GPC was conducted with a Waters 515 pump and Waters 410 differential refractometer using PSS columns (Styrogel 105, 103, 102 Å) with tetrahydrofuran (THF) as an eluent at a flow rate of 1 mL/min (35 °C). Poly(methyl methacrylate) (PMMA) was used as a calibration standard via the WinGPC software from Polymer Standards Service. ^{1}H NMR spectra were obtained using a BRUKER ARX-400 spectrometer and a Bruker 300 MHz spectrometer. UV spectra were obtained from a Guided Wave Model 260 (Guided Wave, Inc., USA) and the fluorescence was measured with a luminescence spectrometer (PerkinElmer, Model LS55). Differential scanning calorimetry (DSC) measurements were performed on a Perkin–Elmer DSC7 at a heating rate of 20 °C/min under a nitrogen atmosphere. The sample was placed in an aluminum pan, sealed tightly, and scanned from 20 to 350 °C. Scanning electron microscope (SEM) images were obtained with a field emission scanning electron microscope (FE-SEM, Hitachi, Model S-4200).

2.3. Synthesis of Fluorophore-Containing Methacrylate Monomers (AntMA: 1 and PyMA: 2)

9-Anthracenemethanol (4.5 g; 0.022 mol) was added to a solution of triethylamine (9.0 mL; 0.065 mol) in 250 mL of anhydrous MC. Methacryloyl chloride (6.3 mL; 0.065 mol) was added dropwise under stirring at 0 °C. The reaction was then conducted at room temperature overnight, after which the reaction medium was filtered. The solvent was evaporated, and the solid residue was purified by recrystallization in 95% ethanol at 40 °C (yield = 90%). 1H NMR ($CDCl_3$), δ ppm: 7.45–8.50 (*m*, 9H, aromatic H), 6.20 (*s*, 2H, CH_2O), 6.05 (*s*, 1H, CH_2 = C), 5.56 (*s*, 1H, CH_2 = C), 1.97 (*s*, 3H, CH_3). Methacrylate monomer containing pyrene (PyMA) was synthesized as previously reported.[14]

2.4. Synthesis of the PMMA Macroinitiator (3)

As an example, $CuCl_2$ (3.79 mg, 0.028 mmol), PMDETA (0.045 ml, 0.022 mmol) and methyl methacrylate (3 ml, 0.028 mol) were mixed in a 3 mL anisole. The mixture was degassed three times using the freeze-pump-thaw procedure and sealed under vacuum. Then, Cu(I)Cl (0.019 g, 0.188 mmol) and a EBiB initiator (0.028 ml, 0.188 mmol) were added to the mixture. The mixture was placed in a preheated oil bath (60 °C) for 1.5 h. The solution was passed through a neutral Al_2O_3 column with THF as an eluent to remove the catalyst. The light yellow filtrate was concentrated under reduced pressure and reprecipitated into methanol. The PMMA was collected by filtration and dried under vacuum. Yield: 70%. M_n (GPC) = 8,700; M_w/M_n = 1.16 (GPC). The resulting PMMA was used as the macroinitiator.

2.5. Synthesis of the Random Copolymer (4)

Antracene containing random copolymer was easily synthesized by copolymerizing a mixture of MMA and AntMA. The composition of the copolymer could be controlled by varying the feed ratio between MMA and AntMA. $CuBr_2$ (4.4 mg, 0.02 mmol), PMDETA (0.07 ml, 0.33 mmol), MMA (1.26 ml, 0.012 mol), and AntMA (**1**) (0.35 g, 1.32 mmol) were mixed in a 1.5 mL anisole. The feed ratio of [MMA]/[AntMA] was changed from 9:1 to 5:1 and 1:1. The mixture was degassed three times using the freeze-pump-thaw procedure and sealed under

vacuum. Then, Cu(I)Br (0.019 g, 0.188 mmol) and the EBiB initiator (0.019 ml, 0.13 mmol) were added to the mixture. The mixture was placed in a preheated oil bath (60 °C) for 2.5 h. The solution was passed through a neutral Al_2O_3 column with THF as an eluent to remove the catalyst. The light yellow filtrate was concentrated under reduced pressure and reprecipitated into ether. The random copolymer was collected by filtration and dried under vacuum. These samples are denoted as P(MMA_{147}-*r*-Ant_{14}), P(MMA_{72}-*r*-Ant_{17}), P(MMA_{17}-*r*-Ant_{13}), where the two numbers indicate the numbers of MMA and AntMA units. M_n (GPC) = 21,900, 11,900, and 5,400; M_w/M_n = 1.17, 1.31, and 1.28 (GPC).

2.6. Synthesis of the Diblock Copolymer (5 and 6)

As an example, $CuBr_2$ (0.45 mg, 0.002 mmol), PMDETA (0.003 ml, 0.015 mmol), PMMA macroinitiator (0.388 g, 0.013 mmol) and AntMA (0.2 g, 0.66 mmol) were mixed in a 2 mL anisole. The mixture was degassed three times using the freeze-pump-thaw procedure and sealed under vacuum. Then, Cu(I)Br (0.0019 g, 0.013 mmol) was added to the mixture. The mixture was placed in a preheated oil bath (90 °C) for 24 h. The solution was passed through a neutral Al_2O_3 column with THF as the eluent to remove the catalyst. The light yellow filtrate was concentrated under reduced pressure and reprecipitated into ether. The diblock copolymer was collected by filtration and dried under vacuum. M_n (GPC) = 9,600; M_w/M_n = 1.16 (GPC). This sample is denoted as $PMMA_{85}$-*b*-$PAnt_{29}$, where the two numbers indicate the number of MMA and anthracene units. To synthesize the block copolymer containing both antracene and pyrene units, antracene containing random copolymer, P(MMA_{91}-*r*-Ant_{11}), as a macroinitiator was reacted with PyMA (2). As a result, a multi copolymer of anthracene random copolymer unit and pyrene block unit, P(MMA_{91}-*r*-Ant_{11})-*b*-Py_{31}, was synthesized. M_n (GPC) = 14,700; M_w/M_n = 1.25 (GPC).

2.7. Fabrication of Fluorescent Nanoporous Films and Nanoscale Micelle Structures Using Diblock Copolymers

Polymer thin films were prepared by the drop-casting method on silicon wafers for SEM measurements. The film thickness could be controlled by changing the volume and concentration of the copolymer solution. To fabricate a fluorescent nanoscale micelle structure, water was slowly added to the diblock copolymer solution in THF. The average size of the micelle structures could be controlled from 130 to 360 nm by changing the water content.

3. RESULTS AND DISCUSSION

3.1. Synthesis and Characterization

9-Anthracenemethyl methacrylate (AntMA) or 1-pyrenemethyl methacrylate (PyMA) containing block copolymers were employed to fabricate nanostructures such as a nanoporous film and micelle particles. To synthesize well-defined fluorescent random and block copolymers, ATRP was conducted with MMA and either AntMA or PyMA, respectively. Scheme 1 shows the synthesis route of AntMA and PyMA as monomers (**1** and **2**),[22] PMMA as the macroinitiator (**3**), AntMA containing random copolymer (**4**), AntMA containing block copolymer (**5**), and a multicopolymer of randomly connected AntMA polymer unit and PyMA block unit (**6**).

As mentioned above, antracene containing random copolymers with different compositions (**4a–c**), P(MMA_{147}-*r*-Ant_{14}), P(MMA_{72}-*r*-Ant_{17}), and P(MMA_{17}-*r*-Ant_{13}), were synthesized with various feed ratios of the two monomers, MMA and AntMA, in order to adjust the composition of the antracene unit. For the synthesis of antracene containing diblock copolymer, the PMMA macroinitiator was first prepared with a molecular weight (M_w) of 8,700 g/mol^{-1} and then used to synthesize antracene containing diblock copolymer (**5**) of relatively narrow polydispersity (PDI = 1.12), $PMMA_{85}$-*b*-Ant_{29}, through ATRP using AntMA. Additionally, the copolymers having both randomly positioned antracene unit and pyrene block unit, (**6**) P(MMA_{91}-*r*-Ant_{11})-*b*-Py_{31}, were synthesized using antracene containing random copolymer, P(MMA_{91}-*r*-Ant_{11}), as a macroinitiator and PyMA (**2**) as a second monomer.

The chemical structure of the monomer, random copolymer, and diblock copolymer were confirmed with ^{1}H-NMR (data now shown). The polymerization was confirmed with the disappearance of the proton resonance in the CH_2=CH double bond for the methacrylate at 6.14 and 5.50 ppm using ^{1}H-NMR. Interestingly, the aromatic proton resonance for the anthracenyl and pyrenyl units in the block copolymer shifted by 0.25 and 0.40 ppm compared to those for the monomers, respectively, possibly because of the strong electronic interaction between the tightly packed aromatic groups in the block copolymers.

The molecular weights of copolymers containing AntMA and PyMA (**4, 5,** and **6**) were determined by GPC using THF as the mobile phase and PMMA standards (Fig. 1). As shown in the GPC trace of Figure 1(a), the M_n of AntMA containing random copolymer gradually increased as a function of the polymerization time, indicating successful growth of polymer chain. The AntMA content of the random copolymers (**4**) was analyzed as 14, 17, and 13 by GPC and ^{1}H-NMR, while the MMA content was 147, 72, and 17, respectively. This result indicates the composition of the random copolymers could be easily modulated by changing the feed ratio of the two monomers (MMA and AntMA). Thus, these random copolymers are indicated as P(MMA_{147}-*r*-Ant_{14}), P(MMA_{72}-*r*-Ant_{17}), and P(MMA_{17}-*r*-Ant_{13}), respectively. As shown in Figures 1(b and c), a shift in the GPC trace of AntMA or PyMA containing diblock copolymers (**5** and **6**) toward higher molecular weight regions

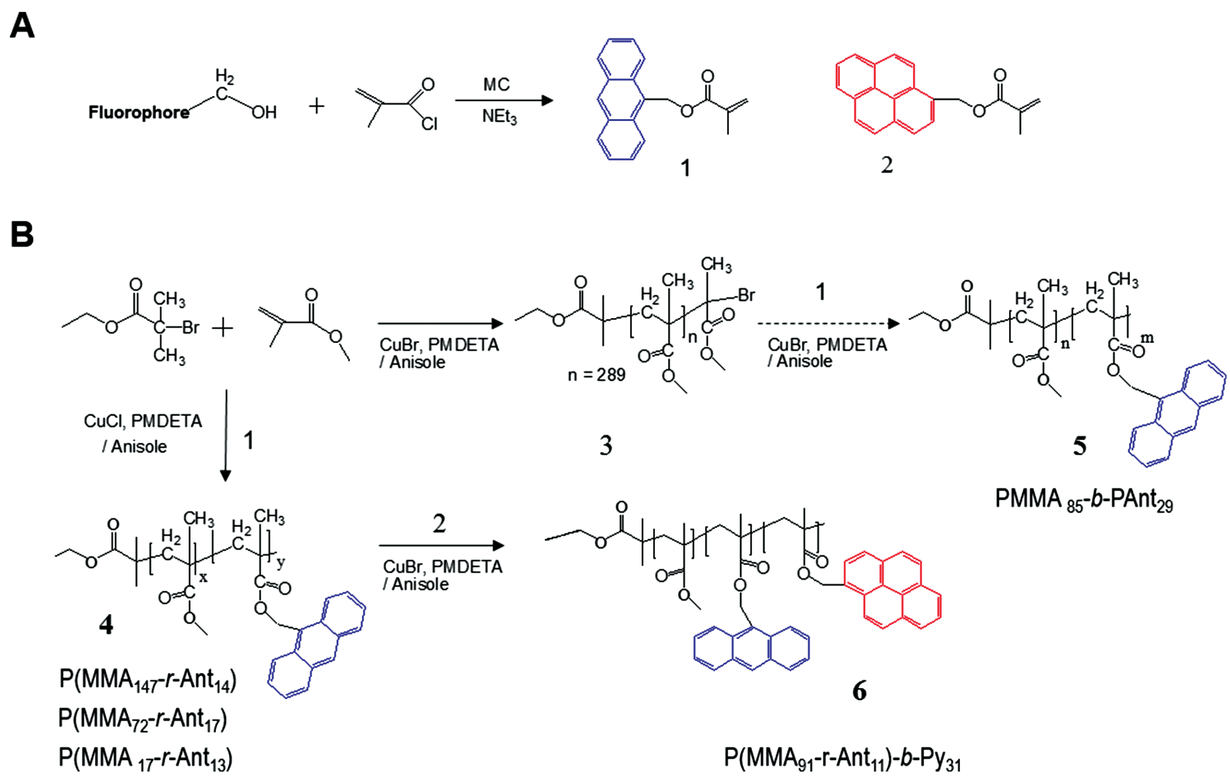

Scheme 1. (A) Synthesis of fluorophore monomers (**1** and **2**). (B) Synthesis of random copolymers and block copolymers containing fluorophores (**4, 5, 6**) via ATRP using the fluorophore monomers (**1** and **2**) and macroinitiators (**3** and **4**).

demonstrates the addition of the AntMA or PyMA block to the PMMA macroinitiator or the AntMA containing random copolymer macroinitiator, respectively. The PDI of diblock copolymers (**5** and **6**) were 1.12 and 1.25, indicating a well-controlled polymerization process. The thermal properties of the random and block copolymers were examined by DSC analysis. The molecular weight, PDI, and optical properties of the random and block copolymers are summarized in Table I. Figure 2(a) shows that the glass-transition temperatures (T_g) in the random copolymers (**4**) increased as the content ratio of MMA to AntMA gradually changed from 10.3:1.0 (**4a**) to 1.3:1.0 (**4c**). The higher T_g in the random copolymer (**4c**) having a MMA:AntMA ratio of 1.3:1.0 may be attributed to stronger interaction between the anthracene groups. More importantly, the anthracene containing block copolymer (**5**) showed two T_g values at 127 and 200 °C, corresponding to PMMA and antracene block segments, respectively, while all random copolymers (**4**) showed a single T_g value. This result also supports the formation of a diblock copolymer composed of PMMA and AntMA block segments.

3.2. Fluorescent Nanostructures by Self-Assembly

The thin films of the random copolymer (**4**) and block copolymer (**5**) were prepared by a drop-casting method with the polymer solutions (2.5 mg/ml in THF). As shown in the SEM images in Figure 3, all random copolymers (**4**) did not show any ordered structures even at a

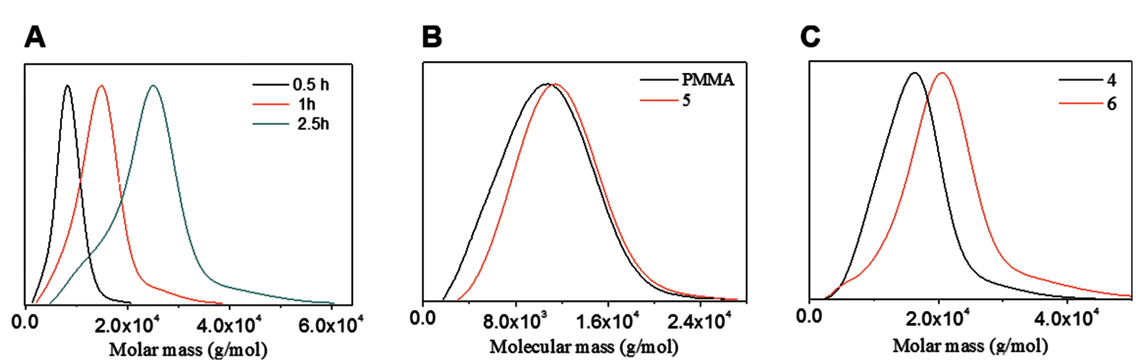

Figure 1. GPC traces of (A) antracene containing random copolymer [P(MMA$_{147}$-*r*-Ant$_{14}$), **4a**], (B) Antracene-containing block copolymer [PMMA$_{85}$-*b*-PAnt$_{29}$, **5**], and (C) a multicopolymer of antracene copolymer and pyrene block [P(MMA$_{91}$-*r*-Ant$_{11}$)-*b*-Py$_{31}$, **6**].

Table I. Summary of the polymerization of random and block copolymers and their optical properties.

Polymer	GPC results	MMA/Fl ratio	λ_{abs}	λ_{emi}	Q. Y.[a]
P(MMA$_{147}$-*r*-Ant$_{14}$), **4a**	M_n = 21900, PDI = 1.17	10.3:1.0	350, 367, 388	398, 416, 439	0.65
P(MMA$_{72}$-*r*-Ant$_{17}$), **4b**	M_n = 11900, PDI = 1.31	4.2:1.0	350, 367, 388	398, 416, 439	0.20
P(MMA$_{17}$-*r*-Ant$_{13}$), **4c**	M_n = 5400, PDI = 1.28	1.3:1.0	350, 367, 388	398, 416, 439	0.07
PMMA$_{85}$-*b*-PAnt$_{29}$, **5**	M_n = 9600, PDI= 1.12	2.9:1.0	350, 369, 389	400, 419, 442	0.24
P(MMA$_{91}$-*r*-Ant$_{11}$)-*b*-Py$_{31}$, **6**	M_n = 14700, PDI = 1.25	8.3:1.0 (AntMA) 2.9:1.0 (PyMA)	278, 314, 340, 345, 367, 388	398, 416, 442, 482	0.17

Notes: [a]Quantum Yield Reference = Antracene in an ethanol solution (0.24).

higher AntMA composition ratio in the random copolymer, P(MMA$_{17}$-*r*-Ant$_{13}$). Alternatively, the block copolymer (**5**) film showed a well-ordered nanoporous structure with a 300–400 nm diameter originating from much stronger self-assembly of the tightly-packed AntMA block unit. Such a dramatic difference between the random and block copolymers in terms of nanostucture formation is due to the self-assembly of closely bound anthracene units in the block copolymer. It is unlikely that such self-assembly would occur in the random copolymer because of the randomly distributed anthracene molecules, which are separated randomly by the MMA units in the random copolymer.

The mechanism on the formation of the pore morphology can be explained based on solvent-induced breath figure formation, as previously described.[23,24] Briefly, the diblock copolymers form a disordered phase in dilute solution upon casting (Fig. 3(d)). As the solvent is evaporated and temperature drops upon solvent evaporation, the diblock copolymers tend to form spherical micelles, consisting of a core and a corona (possibly of the hydrophobic anthracene blocks). After subsequent evaporation of the solvent, polymer films with ordered pore patterns could be generated as the THF solvent molecules filled inside gaps leave upon evaporation. The nanopore sizes could be modulated by several factors, including M_n and the composition ratio of diblock copolymers, as previously reported.[25,26] Similar to the block copolymer containing AntMA (**5**), the block copolymer (**6**) with the PyMA block unit also exhibited clear a nanopore structure with a 200–350 nm diameter size, due to the stronger self-assembly of the closely bound pyrene units, as shown in Figure 4(a). Compared to the AntMA containing block copolymer (M_n = 9600, **5**), the PyMA containing block copolymer (M_n = 14700, **6**) film showed a smaller pore size, which might be mainly due to the larger molecular weight of the PyMA block copolymer.

Another fluorescent nanoscale micelle structure (200 nm diameter) of the block copolymers (**6**) was observed when the poor solvent (water) for the PyMA groups was slowly added to its solution in THF. This is attributed to the strong hydrophobic interactions of pyrene units, which may allow self-assembly of the pyrene units as shown in Figure 4(b).

3.3. Photophysical Properties

Figures 5(a and b) shows the UV-Vis absorption and emission (PL) spectra of the AntMA monomer, AntMA containing random and block copolymers (**4** and **5**) in chloroform. The absorption spectra of the AntMA monomer exhibited three vibronic bands at 342, 359, and 378 nm corresponding to the electronic transition of the anthracene molecule. Compared to the AntMA monomer, the random and block copolymers (**4** and **5**) in solution showed red shifted absorption peaks at 350, 367, and 388 nm, possibly due to the association of anthracene resulting from the polymer structures. The PL spectra of the random copolymers (**4**) showed three sharp peaks at 398, 416 and 439 nm, which are assigned to the anthracene unit. Alternatively, the PL spectrum of the block copolymer (**5**) showed slightly red-shifted peaks at 400, 419, and 442 nm with a broad tailing of the peak reaching

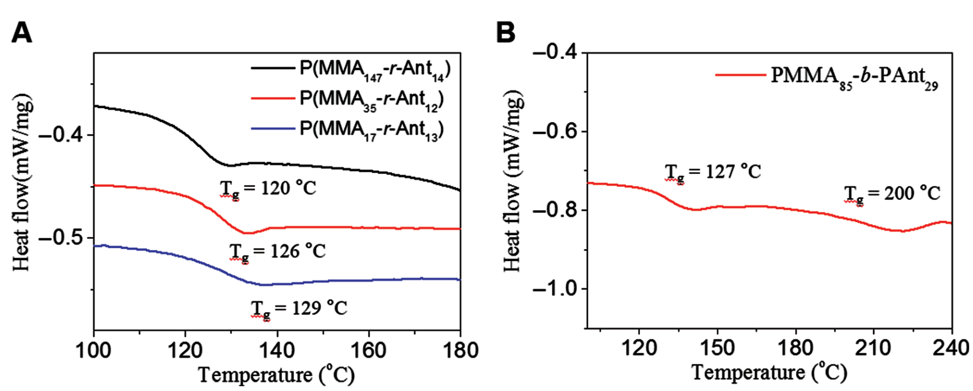

Figure 2. DSC thermogram of (A) antracene-containing random copolymer, P(MMA$_{147}$-*r*-Ant$_{14}$, **4a**), P(MMA$_{35}$-*r*-Ant$_{12}$, 4b), P(MMA$_{17}$-*r*-Ant$_{13}$, **4c**) and (B) antracene-containing block copolymer, PMMA $_{85}$-*b*-PAnt$_{29}$ (**5**).

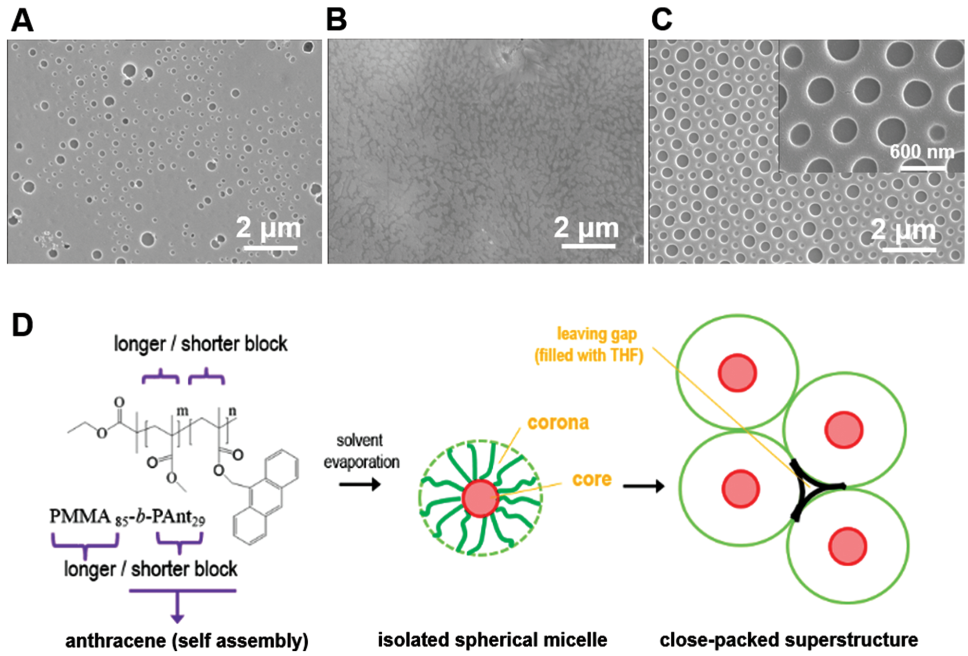

Figure 3. SEM images of the films of (A) P(MMA_{147}-*r*-Ant_{14}), (B) P(MMA $_{17}$-*r*-Ant_{13}), and (C) PMMA $_{85}$-*b*-$PAnt_{29}$ by drop casting onto silicon wafers (inset: magnified image). (D) Schematic illustration for nanopore formation of antracene-containing block copolymer (**5**) via solvent-induced pore patterning.

~550 nm. This is likely due to the unique block copolymer structures where anthracene groups exist in close proximity, leading to strong π–π interactions. Figure 5(c) reveals that the quantum yield (Φ_E) of anthracene containing copolymers (**4**) was dependent on the feed ratio between MMA and AntMA composition. The random copolymer with a higher ratio of MMA to AntMA, P(MMA_{147}-*r*-Ant_{14}), showed a larger Φ_E of 65%. Alternatively, the random copolymers with a lower MMA to AntMA ratio, such as P(MMA_{72}-*r*-Ant_{17}) and P(MMA_{17}-*r*-Ant_{13}), showed much lower quantum yields (20% and 7%, respectively) compared to that of P(MMA_{147}-*r*-Ant_{14}). The association of anthracene fluorophores tends to quench the emission and reduce the quantum yield. Interestingly, the Φ_E value of the block copolymer (**5**) was 24% in spite of the densely packed anthracene units within the block segment. The higher Φ_E value of the block copolymer (**5**) might be ascribed to the well-ordered anthracene block unit, to lead

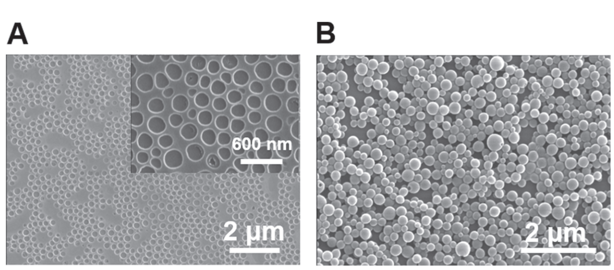

Figure 4. FE-SEM images of (A) the film of P(MMA_{91}- *r*-Ant_{11})-*b*-Py_{31} by drop casting onto silicon wafers (inset: magnified image) and (B) micelle structure of P(MMA_{91}-*r*-Ant_{11})-*b*-Py_{31} by the addition of poor water solution to dilute THF solution.

aggregation induced emission enhancement,[27,28] while the high content of anthracene in the random copolymers, without ordering of the anthracene units, lead concentration quenching.[29,30] Figure 6 shows the UV-vis and emission spectra of a multiple copolymer (**6**), P(MMA_{91}-*r*-Ant_{11})-*b*-Py_{31}, which consists of random MMA:AntMA and block PyMA unit. As shown in Figure 6(a), absorption bands at 278, 314, and 340 nm originated from the pyrene group while other bands at 345, 367, and 388 nm resulted from the anthracene group. Interestingly, as shown in Figure 6(b), the PL spectrum of the block copolymer (**6**) shows the contribution of both fluorophores, anthracene and pyrene, as a function of the excitation wavelength. The sharp anthracene emissions at 398, 417, and 442 nm as well as the pyrene excimer emission at 482 nm were obtained at the same time upon excitation at 360 nm.

Figure 7 shows emission spectra of nanostructures, both nanoporous films and micelle solutions, formed by fluorophore containing block copolymers (**5**, and **6**). In contrast to their solution-state conditions (Figs. 5 and 6), nanoporous structures exhibited much broader emission bands, due to the highly aggregated fluorophores in films (Fig. 7(a)). Interestingly, the film of the P(MMA_{91}-*r*-Ant_{11})-*b*-Py_{31} block copolymer (**6**) showed broader emission band with red-shifted emission compared to the anthracene block copolymers (**5**). Moreover, as shown in Figure 7(b), the emission spectra of micelle solution (**6**) revealed increased pyrene excimer peaks under all excitation wavelength compared to those of **6** in dilute solution, in which micelle formation must be unfavorable (Fig. 6(b)). This is because pyrenes can interact closely

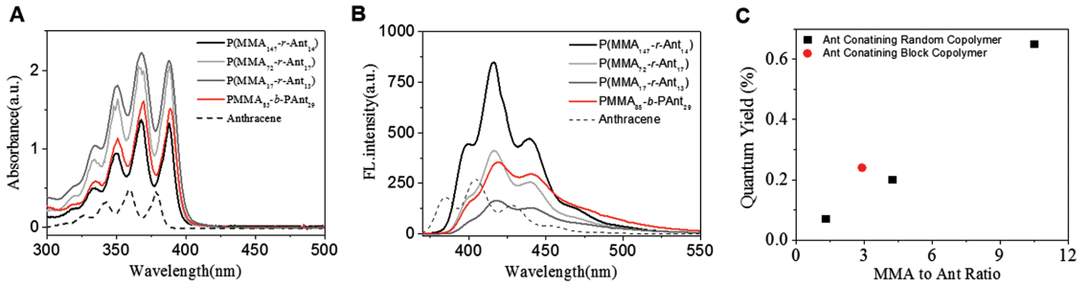

Figure 5. (A and B) UV-vis and emission spectra of several P(MMA-*r*-Ant) copolymers (**4a–c**) (0.25 mgml^{-1}), P(MMA-*b*-AntMA) block copolymer (**5**) (0.25 mgml^{-1}), the antracene monomer (5.6×10^{-5}M) in a chloroform solution ($\lambda_{exc} = 350$ nm). (C) Quantum yield of the random and block copolymer containing antracene as a function of the feed ratio between MMA and AntMA.

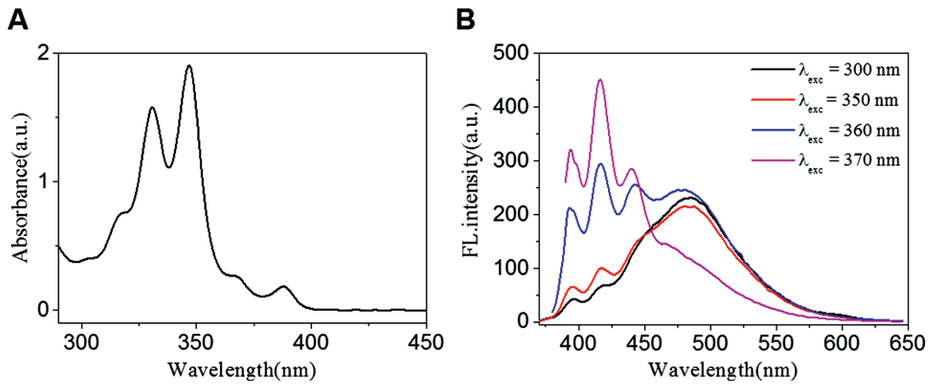

Figure 6. (A) UV-vis and (B) emission spectra of P(MMA$_{91}$-*r*-Ant$_{11}$)-*b*-Py$_{31}$ (0.05 mgml^{-1}).

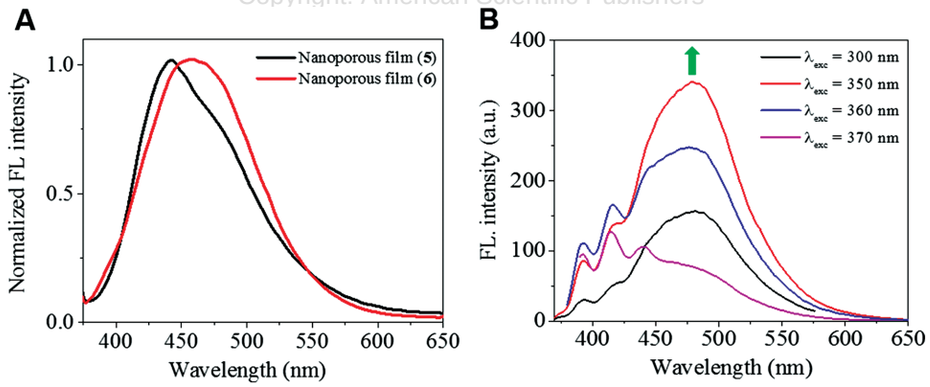

Figure 7. Emission spectra of fluorescent nanostructures, (A) nanoporous films (**5, 6**), PMMA$_{85}$-*b*-PAnt$_{29}$, and P(MMA$_{91}$-*r*-Ant$_{11}$)-*b*-Py$_{31}$, ($\lambda_{exc} = 350$ nm) and (B) micelle solution (**6**), P(MMA$_{91}$-*r*-Ant$_{11}$)-*b*-Py$_{31}$.

in a core part inside micelle structures. Thus, the micelle solution (**6**) exhibited much higher fluorescence intensity ratio of pyrene excimer to anthracene emission (I_{PE}/I_{An}) (determined by the intensities of the pyrene excimer emission at its maximum at 480 nm and that of the anthracene at 415 nm). Under the excitation at 360 nm, the I_{PE}/I_{An} ratio of the micelle condition was determined as 1.50, which is ~1.8 times higher than that in the dilute solution state. Therefore formation of block and content of a fluorescent unit in the copolymer provide a method to tune the emission intensity as well as color (peak) and nanostructure of a fluorescent polymer film. The polymer micelle structure is a promising material for the applications of nanocarrier systems and biosensor devices. Future studies will attempt to study the mechanism to control the size and distribution of fluorescent nanostructures.

4. CONCLUSION

In order to modulate the unique physicochemical properties of the nanostructured materials, including the electronic and photonic functions, it is necessary to

establish precise synthetic methods to enable control of the chemical structures and the composition of each functional unit, polymer chain length, and polydispersity. In this study, we designed and synthesized well-defined fluorescent block and random copolymers via ATRP with a fluorophore (antracene or pyrene) bound methacrylate. The random copolymers contained randomly connected fluorephore units by covalent chemical bonding, in which fluorephore units are separated by MMA units. On the other hand, the fluorophore diblock copolymers was consist of a fluorophore (AntMA or PyMA) block, in which fluorophore units are connected consecutively, and a PMMA macromer. The random copolymer of MMA and AntMA could be connected further to PyMA polymer in which fluorophorescent PyMA units are connected consecutively to form a block copolymer. The composition and distribution of the fluorophores in random and block copolymers was easily adjusted by controlling the monomer feed ratios, macroinitiators, and second monomers. These random and block copolymers show different thermal and optical properties based on their structures and compositions. More importantly, we successfully fabricated fluorescent nanostructures, such as nanoporous films and micelle structures, by self-assembly of block copolymers. This study describing well-defined fluorophore containing copolymers informs the development of novel functional nanostructures for various optoelectronic and biomedical applications.

Acknowledgments: This work was supported by the financial support of the National Research Foundation (NRF) grant funded by the Korea government (MSIP) (R11-2007-005609), the Korea Health Industry Development Institute (KHIDI), funded by the Ministry of Health & Welfare (grant number: HI15C0942), and a grant from Kyung Hee University in 2015 (KHU-20150511).

References and Notes

1. H. Hu, M. Gopinadhan, and C. O. Osuji, *Soft Matter* 10, 3867 (**2014**).
2. G. M. Whitesides, J. P. Mathias, and C. T. Seto, *Science* 254, 1312 (**1991**).
3. C. T. Kresge, M. E. Leonowics, W. J. Roth, J. C. Vartuli, and J. S. Beck, *Nature* 359, 710 (**1992**).
4. A. Sayari, *Chem. Mater.* 8, 1840 (**1996**).
5. J. E. G. J. Wijnhoven and W. L. Vos, *Science* 281, 802 (**1998**).
6. A. Imhor and D. J. Pine, *Nature* 389, 948 (**1997**).
7. J. D. Giannopoulos, P. R. Villeneuve, and S. Fan, *Nature* 386, 143 (**1997**).
8. Y. S. Zhao, H. Fu, A. Peng, Y. Ma, Q. Liao, and J. Yao, *Acc. Chem. Res.* 43, 409 (**2010**).
9. S. Moungthai, N. Mahadevapuram, P. Ruchhoeft, and G. E. Stein, *ACS Appl. Mater. Interfaces* 4, 4015 (**2012**).
10. S. Tu, S. H. Kim, J. Joseph, D. A. Modarelli, and J. R. Parquette, *J. Am. Chem. Soc.* 133, 19125 (**2011**).
11. J. Kim, B. Kim, C. Anand, A. Mano, J. S. M. Zaidi, K. Ariga, J. You, A. Vinu, and E. Kim, *Angew. Chem. Int. Edit.* 54, 8407 (**2015**).
12. T. Park, J. You, H. Oikawa, and E. Kim, *J. Nanosci. Nanotechnol.* 14, 8678 (**2014**).
13. J. You, J. Kim, T. Park, B. Kim, and E. Kim, *Adv. Funct. Mater.* 22, 1417 (**2012**).
14. J. You, J. A. Yoon, J. Kim, C.-F. Huang, K. Matyjaszewski, and E. Kim, *Chem. Mater.* 22, 4426 (**2010**).
15. J. Kim, E. Lee, Y. Hong, B. Kim, M. Ku, D. Heo, J. Choi, J. Na, J. You, S. Haam, Y.-M. Huh, J.-S. Suh, E. Kim, and J. Yang, *Adv. Funct. Mater.* 25, 2260 (**2015**).
16. H.-F. Ji, R. Dabestani, and G. M. Brown, *J. Am. Chem. Soc.* 122, 9306 (**2000**).
17. J. Y. Kwon, N. J. Singh, H. N. Kim, S. K. Kim, S. K. Kim, and J. Yoon, *J. Am. Chem. Soc.* 126, 8892 (**2004**).
18. H. Mori and H. Tanaka, *Macromol. Chem. Phys.* 212, 2349 (**2011**).
19. J.-M. Lu, Q.-F. Xu, X. Yuan, X.-W. Xia, and L.-H. Wang, *J. Polym. Sci. A Polym. Chem.* 45, 3894 (**2007**).
20. J. Kim, C. Anand, S. N. Talapaneni, J. You, S. S. Aldeyab, E. Kim, and A. Vinu, *Angew. Chem. Int. Edit.* 51, 2859 (**2012**).
21. K. Rameshbabu, Y. Kim, T. Kwon, J. Yoo, and E. Kim, *Tetrahedron Letters* 48, 4755 (**2007**).
22. X.-D. Lou, R. Daussin, S. Cuenot, A.-S. Duwez, C. Pagnoulle, C. Detrembleur, C. Bailly, and R. Jérôme, *Chem. Mater.* 16, 4005 (**2004**).
23. K. Ishizu, M. Sugita, H. Kotsubo, and R. Saito, *J. Colloid Interface Sci.* 169, 456 (**1995**).
24. K. Ishizu, Y. Tokuno, and M. Makino, *Macromolecules* 40, 763 (**2007**).
25. M. Srinivasarao, D. Collings, A. Philips, and S. Patel, *Science* 292, 79 (**2001**).
26. H. Yabu and M. Shimomura, *Chem. Mater.* 17, 5231 (**2005**).
27. Y. Jiang, Y. Wang, J. Hua, J. Tang, B. Li, S. Qian, and H. Tian, *Chem. Commun.* 46, 4689 (**2010**).
28. W. Jia, P. Yang, J. Li, Z. Yin, L. Kong, H. Lu, Z. Ge, Y. Wu, X. Hao, and J. Yang, *Polym. Chem.* 5, 2282 (**2014**).
29. R. F. Chen and J. R. Knutson, *Anal Biochem.* 172, 61 (**1988**).
30. A. V. Barzykin, V. F. Razumov, and M. V. Alfimov, *J. Phys. Chem.* 95, 4814 (**1991**).

Received: 20 July 2015. Accepted: 8 March 2016.